Dynamic Rate Adaptation and Integrated Rate and Error Control in Cellular WCDMA Networks

Dong In Kim, *Senior Member, IEEE*, Ekram Hossain, *Member, IEEE*, and Vijay K. Bhargava, *Fellow, IEEE*

***Abstract*—Optimal dynamic rate allocation among mobile stations for variable rate packet data transmission in a cellular wireless network is an NP-complete problem; therefore, suboptimal solutions to this problem are sought for. In this paper, three novel suboptimal dynamic rate adaptation schemes, namely, *peak-interference-based rate allocation*, *sum-interference-based rate allocation*, and *mean-sense approximation-based rate allocation*, are proposed for *uplink* packet data transmission in cellular variable spreading factor wide-band code division multiple access (WCDMA) networks. The performances of these schemes are compared to the performance of the *optimal* dynamic link adaptation for which the rate allocation is found by an exhaustive search. The optimality criterion is the maximization of the average number of radio link level frames transmitted per frame time under constrained signal-to-interference-plus-noise ratio (SINR) at the base station receiver. Two different error control alternatives for variable rate packet transmission environment are presented. We demonstrate that the dynamic rate adaptation problem under constrained SINR can be mapped into the radio link level throughput maximization problem with integrated rate and error control. Performance evaluation is carried out under random and directional micromobility models with uncorrelated and correlated long-term fading, respectively, in a cellular WCDMA environment for both the homogeneous (or uniform) and the nonhomogeneous (or nonuniform) traffic load scenarios.**

***Index Terms*—Dynamic rate adaptation, radio link level error control, wide-band code division multiple access (WCDMA).**

I. Introduction

In CELLULAR wireless networks, adaptive packet access schemes based on dynamic rate and error control can provide superior system performance resulting from higher radio resource utilization. Wide-band code division multiple access (WCDMA) systems (e.g., ETSI WCDMA, cdma2000), which will be the major radio transmission technologies for IMT-2000, have intrinsic support for dynamic rate transmission. In a WCDMA system, with a fixed number of assigned codes, the *uplink* data transmission rate can be controlled on a frame-by-frame basis by using a variable spreading factor (VSF) method [1]–[3].[1] This method for dynamic rate variation is attractive due to its simplicity in implementation and potential for low power consumption at the mobile stations [2].

The problem of dynamic radio link level rate allocation to maximize the average number of transmitted frames per frame time (or channel utilization) under constrained signal-to-interference-plus-noise ratio (SINR) is non-deterministic polynomial (NP)-complete[2] (to be described later in this paper). Therefore, fast and efficient suboptimal solutions to this problem (presumably based on interference and fading conditions) are sought.

In this paper, the problem of dynamic rate adaptation is addressed assuming a single class of users where all the users have a similar quality of service (QoS) requirement in terms of the received SINR at the base station (BS) receiver. Three novel suboptimal dynamic rate adaptation schemes, namely, *peak-interference*-based rate allocation, *sum-interference*-based rate allocation, and *mean-sense approximation*-based rate allocation, are proposed for uplink packet data transmission in cellular variable spreading factor WCDMA networks. The optimality criterion is the maximization of the average number of radio link level frames transmitted per frame time while satisfying the SINR requirements for the mobiles.

Based on a generalized uplink SINR model (applicable to uniform and nonuniform traffic load scenarios in multicell environment) developed considering both the long-term fading and the short-term fading conditions, the performances of the proposed suboptimal rate adaptation schemes are compared to the performance of the *optimal* dynamic link adaptation for which the rate allocations among the mobiles are found by an exhaustive search. Although the *fairness* in radio link level transmission rates among the different mobiles is not posed as an optimization constraint, we also observe the achieved fairness for the different rate adaptation schemes. Performance evaluation is carried out under *random* and *directional* micromobility models with uncorrelated and correlated long-term fading, respectively. Since the short-term fading (i.e., multipath fading) changes more rapidly compared to the long-term fading (i.e., path-loss and shadowing), it is assumed to be independently varying.

A time-framed system is considered here in which the frame duration is fixed. Depending on the rate selection, however, a

Manuscript received September 30, 2001; revised May 30, 2002; accepted October 4, 2002. The editor coordinating the review of this paper and approving it for publication is K. B. Lee. This work was supported in part by the Brain Korea 21 Project and by the Natural Sciences and Engineering Research Council (NSERC), Canada.

D. I. Kim was with the University of Seoul, Seoul, Korea. He is now with the School of Engineering Science, Simon Fraser University, Burnaby, BC V5A 1S6 Canada (e-mail: dikim@sfu.ca).

E. Hossain is with the Department of Electrical and Computer Engineerng, University of Manitoba, Winnipeg, MB R3T 5V6 Canada (e-mail: ekram@ee.umanitoba.ca).

V. K. Bhargava is with the Department of Electrical and Computer Engineering, University of British Columbia, Vancouver, BC V6T 1Z4 Canada (e-mail: vijayb@ece.ubc.ca).

Digital Object Identifier 10.1109/TWC.2003.819039

[1]In a UMTS or 2000 system, the spreading factor and the number of codes in the *downlink* are fixed.

[2]The family of NP-complete problems includes many important optimization problems which are all inherently of exponential time complexity and algorithms for solving them in less than exponential time do not exist.

1536-1276/04$20.00 © 2004 IEEE

mobile station can transmit a variable number of fixed length radio link control (RLC)/medium access control (MAC) layer frames within one frame time, which are derived from the segmentation of variable-length IP packets. In such an environment, dynamic rate adaptation can be integrated with RLC/MAC level error recovery (for example, using channel coding) subsequent to some transmission failure. Two error control schemes are presented which are based on the idea of integrating dynamic rate adpatation with radio link level error control. We demonstrate, in this paper, how the dynamic rate adaptation can be integrated with radio link level error control to optimize the radio link level throughput (in bits/second).

The rest of the paper is organized as follows. Section II reviews the pertinent literature and presents the motivation of this work. An uplink SINR model for multicell VSF WCDMA systems is developed in Section III. In Section IV, the dynamic rate adaptation problem and the radio link level error control methods under variable rate transmission for packet-switched cellular WCDMA systems are described. The suboptimal rate allocation procedures are presented in Section V. In Section VI, the idea of integrated rate and error control under mean-sense approximation-based dynamic rate adaptation is presented. The simulation model and the simulation results are presented in Section VII. Conclusions are stated in Section VIII.

II. Background and Motivation

An adaptive variable transmission rate random access scheme based on direct-sequence CDMA (DS-CDMA) slotted ALOHA (S-ALOHA) in an additive white Gaussian noise (AWGN) environment was proposed in [4], although no rate selection procedure (other than the exhaustive search) was assumed in the presented analytical model.

An adaptive multiple access scheme for uplink admission/congestion control was proposed in [5] for variable spreading gain CDMA systems with variable received power operating in an AWGN environment. The scheme was based on the adaptation of the retransmission control probability for the users with different but fixed transmission rates. The problem of dynamic rate control was not addressed therein.

The effect of dynamic spreading gain control on the dynamics of multiple access interference (MAI) and spectral efficiency in a *single-cell* S-ALOHA system was studied in [6] where all the mobile terminals used similar dynamically varying spreading gain to maximize total system throughput.

In [7], nonreal-time packet-data traffic throughput (in the uplink) was evaluated in a *single-cell* variable spreading gain voice-data CDMA system. The objective was to maximize the average data throughput while minimizing the sum of the transmit powers used by the mobiles.

It was observed that in many cases a time-scheduled transmission mode where only one terminal among all of the data terminals are allowed to transmit at a time, provides remarkably higher per-user throughput compared to the conventional unscheduled (or random) transmission mode. This observation on the throughput-maximizing rate distribution is in line with the information-theoretic results on optimal cellular capacity in [8], which basically state that a necessary condition to maximize system capacity is to separate the users in a cell and share the available bandwidth between cells.

Similar results were obtained in [9], where the throughput maximization problem for CDMA uplinks was formulated as an optimization problem in terms of the spreading gains and transmit power of the users. In the optimal power and rate optimization strategy only one user in a cell that has the most favorable channel condition transmits at the highest possible rate.

This work presented in this paper is different from those in the above in that it addresses the problem of *optimal* dynamic rate adaptation under constrained SINR for uplink packet data transmission in *multicell multirate* WCDMA systems. The optimality criterion is the maximization of the average number of radio link level frames transmitted per frame time. The main contribution of this paper is the formulation of the optimal dynamic rate adaptation problem under constrained SINR using a general SINR model for uplink data transmission in cellular VSF WCDMA networks. In the proposed dynamic rate adaptation framework, the impact of the rate allocations in other cells is taken into consideration and the other-cell interference factors are explicitly taken into consideration (rather than treating all the other-cell interference as noise).

The observations on the throughput maximizing rate distributions in some of the previous works are utilized to devise simple heuristic-based rate adaptation algorithms with reduced computational/implementation complexity (compared to the optimal dynamic rate adaptation). Again, the idea of integrating dynamic rate adaptation with radio link level error control is introduced. Two radio link level error control alternatives for variable rate packet data transmission are presented.

Although the problem of dynamic rate adaptation for packet data service with a single class of users (e.g., best-effort packet data service) has been considered only, the framework can be extended to handle the case with multiple class of users.

III. Modeling of Uplink SINR

To devise radio link level dynamic rate allocation schemes for multicell multirate WCDMA systems, it is required to first develop an effective uplink signal-to-interference-plus-noise ratio (SINR) model. A list of the key mathematical notations is provided in Table I for the SINR model developed below.

Let us assume that the frame time, denoted by T, is fixed and that the transmission rates can be selected from the set of rates $\{r_0, r_1, \ldots, r_\varphi\}$. If it is assumed that $r_m = mr_1$ ($m = 0, 1, \ldots, \varphi$),[3] and that only one frame (of fixed length of M bits) corresponding to the smallest (basic) rate r_1 can be transmitted during a frame time, then for the transmission rate of r_m, m frames can be transmitted during a frame time. For this, a variable spreading gain WCDMA system can be used where the basic gain is given by N chips per bit, and for rate r_m, the spreading gain is reduced to N/m chips per bit.

[3]For the rest of the paper it is assumed that $r_m = mr_1$ so that the normalized value of r_m with respect to the basic rate r_1 is m.

TABLE I
LIST OF KEY NOTATIONS

g_j, $j = 0, \cdots, J$	Number of mobiles in cell j
G	Number of mobiles per cell in case of uniform traffic load
$m_i^{(j)}$	Transmission rate allocated to ith mobile in cell j
$P_{b,i}^{(j)}$	Power allocated to ith mobile in cell j corresponding to the basic rate r_1
$\rho_j(j',k)$	L-path fading corresponding to the link between $(BS)_j$ and kth mobile in cell j'
$L_j(j',k)$	Long-term fading corresponding to the link between $(BS)_j$ and kth mobile in cell j'
$m_i^{(j)} \times P_{b,i}^{(j)}$	Total power allocated to ith mobile in cell j
P_b	Received signal power at the BS corresponding to the basic transmission rate r_1
$\eta_{j'/j}(k)$	Other-cell interference factor in cell j corresponding to transmission from kth mobile in cell j'
$(SINR)_{o,i}^{(j)}$	Output SINR correponding to ith mobile in cell j
$(SINR)_o$	Target SINR
$\bar{\eta}_j$	Average other-cell interference factor in cell j
x	Effective traffic load
$p_{b,m}$	Bit error rate for a user with rate r_m
$p_{c,m}$	Probability of correct frame reception for a user transmitting at rate r_m
β	Radio link level throughput, frames/frame time

For this, mutually orthogonal codes (e.g., orthogonal variable spreading factor (OVSF) codes[4] [1]) for different transmission rates are possible if a rate r is chosen according to

$$\frac{r}{r_1} = \frac{N}{2^n}, \quad n = 0, 1, \ldots, \log_2 N \tag{1}$$

where $2^n = N$ is the basic spreading gain (in chips/bit) corresponding to $r = r_1$. This results in a variable rate resolution which becomes very coarse for relatively higher transmission rates. The highest transmission rate (r_φ) would be presumably limited by some minimum required spreading gain. For a constant rate resolution, nonorthogonal spreading codes must be used as a consequence of which the intracell interference will be increased.

Assuming random signatures and considering both the short-term L-path Rayleigh fading and the long-term fading, i.e., path-loss and shadowing, the RAKE-combined output SINR at the jth base station, $(\mathrm{BS})_j$ corresponding to the transmission from ith mobile in cell j ($j = 0, 1, \ldots, J$) can be expressed by (2). Here, $\rho_j(j',k) = \sum_{l=1}^{L} a_{j,k(j'),l}^2$ represents the L-path multipath fading gain with $a_{j,k(j'),l}$ being the path gain between $(\mathrm{BS})_j$ and the kth mobile in cell j' corresponding to the lth path, and $L_j(j',k)$ represents the long-term fading for the same link

$$(\mathrm{SINR})_{o,i}^{(j)} = \frac{\rho_j(j,i)(m_i^{(j)} P_{b,i}^{(j)}) \left(\frac{T_b}{m_i^{(j)}}\right) L_j(j,i)}{\frac{1}{3}\sum_{j'=0}^{J}\sum_{k=1}^{g_{j'}} m_k^{(j')} P_{b,k}^{(j')} T_c \rho_j(j',k) L_j(j',k) + \frac{N_o}{2}}. \tag{2}$$

$L_j(j',k)$ is defined by

$$L_j(j',k) = d_{j,k(j')}^{-\delta} \cdot 10^{\xi_{j,k(j')}/10} \tag{3}$$

where the signal is assumed to be attenuated by the δth power of the distance $d_{j,k(j')}$ and log-normal shadowing with standard deviation σ.

In (2), $m_i^{(j)} \in \{0, 1, \ldots, \varphi\}$ denotes a specific rate allocation to the ith mobile in cell j, $P_{b,i}^{(j)}$ is its transmit power at basic rate, and $mP_{b,i}^{(j)}$ is transmit power with rate r_m ($m = m_i^{(j)}$) where the bit time T_b is reduced to T_b/m because of the VSF scheme. In (2), the factor 1/3 results from the rectangular chip pulse and uniform delay distribution for a chip time T_c [10], $g_{j'}$ is the number of mobiles in cell j', and $N_o/2$ is the power spectral density of the background noise.

Note that when we derive the lth path $(\mathrm{SINR})_{o,i,l}^{(j)}$ (where $\sum_{l=1}^{L}(\mathrm{SINR})_{o,i,l}^{(j)} = (\mathrm{SINR})_{o,i}^{(j)}$), $\rho_j(j',k)$ in (2) is to be replaced by $\rho_j(j,i) - a_{j,i(j),l}^2$ in case of $j' = j$ and $k = i$. This is because the self-interference due to delayed multipath signals from the ith mobile in cell j does not include the desired lth path signal. Compared to the total in-cell and other-cell interferences, its effect is typically negligible and therefore (2) can be regarded as a conservative estimate for the unified SINR analysis.

In general, the uplink channel is power controlled to normalize the received signal power at basic rate. The received signal power at $(\mathrm{BS})_j$, which is constant for all mobiles in the same cell, can be expressed as

$$P_b = \rho_j(j,i) P_{b,i}^{(j)} L_j(j,i) \tag{4}$$

for $i = 1, \ldots, g_j$ and $j = 0, 1, \ldots, J$.

Using (4), the RAKE-combined output SINR in (2) can be formulated as

$$(\mathrm{SINR})_{o,i}^{(j)} = \left[\frac{1}{3N}\sum_{k=1}^{g_j} m_k^{(j)} + \frac{1}{3N}\sum_{j'\neq j}\sum_{k=1}^{g_{j'}} m_k^{(j')} \eta_{j'/j}(k) + \left(\frac{2E_b}{N_o}\right)^{-1}\right]^{-1} \tag{5}$$

where $E_b = P_b T_b$ is the bit energy, $N = T_b/T_c$ denotes the spreading factor at basic rate, and $\eta_{j'/j}(k)$ is the other-cell interference factor defined as follows:

$$\eta_{j'/j}(k) \triangleq \frac{\rho_j(j',k) L_j(j',k)}{\rho_{j'}(j',k) L_{j'}(j',k)}. \tag{6}$$

In (5), the first term represents the sum of the transmission rates in cell j, the second and third terms denote the other-cell interference weighted by the corresponding rate distributions and the output signal-to-noise ratio (SNR) per bit, respectively.

The important observation here is that the rate allocation in one cell affects the rate allocation in other cells, because when higher rates are allocated to mobiles in one cell, it increases the

[4]OVSF codes for variable rate transmission can be generated from the subset of row vectors in the Hadamard matrix H_n of size $2^n \times 2^n$ (n is an integer). The maximum value of 2^n would be roughly of the order of the number of users supportable in a cell.

other-cell interference and in turn reduces the sum of the transmission rates in other cells because of the weighting effect in the second term in the expression for SINR in (5). This implies that the dynamic rate allocation should be performed jointly over all the cells involved to minimize the other-cell interference and hence maximize the sum of the radio link level transmission rates.

IV. Dynamic Rate and Error Control

A. Optimal Dynamic Rate Allocation

Based on the uplink SINR modeling developed in Section III, an optimal rate allocation can be defined as follows:

$$\text{choose } \max\left\{\sum_{j=0}^{J}\sum_{i=1}^{g_j} m_i^{(j)}\right\}$$
$$\text{subject to } (\text{SINR})_{o,i}^{(j)} \geq (\text{SINR})_o \text{ for all } i \text{ and } j \qquad (7)$$

assuming all mobiles require the same uplink quality across the cells, or equivalently, the same SINR constraint (with target $(\text{SINR})_o$) applies to all mobiles in all the cells.

Note that the optimal rate allocation can be determined by an exhaustive search to find the rate combinations $\{m_i^{(j)} \mid i = 1,\ldots,g_j;\ j = 0,1,\ldots,J\}$ that maximizes the sum of the transmission rates within the SINR constraint in (7). Since the exhaustive search requires cycling through all possible assignments which would involve exponential time complexity (with the order of the complexity being $O\left(\prod_{j=0}^{J} g_j^{(1+\varphi)}\right)$), the problem of optimal rate allocation (which is similar to the *satisfiability problem* [11, p. 673]) is NP-complete. Therefore, it is unlikely that a true optimal algorithm for this problem (other than the exhaustive search) exists. Hence, in a practical scenario, a fast and efficient procedure would be desirable which may not necessarily result in true optimal rate allocation but a suboptimal rate allocation.

B. Suboptimal Dynamic Rate Allocation and Performance Measures

In Section V of this paper, we propose two suboptimal "joint-cell" rate adaptation schemes, namely, *peak-interference-based rate allocation* and *sum-interference-based rate allocation* which have linear complexity of $O\left(\sum_{j=0}^{J} g_j\right)$. However, these two suboptimal schemes would require the radio network controller (RNC) to estimate all the other-cell interference factors $\{\eta_{j'/j}(k)\}$ [in (6)] corresponding to all the mobiles in all the cells and, therefore, may cause large network overhead. For this reason, we also propose a single-cell *mean-sense approximation-based* dynamic rate allocation procedure as a promising alternative to the joint-cell rate allocation in view of both the performance and implementation. In this case, the other-cell interference in a target cell is accounted for in an average sense.

The performance measures considered for the different rate adaptation algorithms are *average transmission rate* per mobile per frame time ($E(m_i^{(j)})$) under constrained SINR and *(intercell) fairness* (F_{inter}) in the average transmission rate among the different mobiles in the different cells. The *intercell fairness* among $E(m_i^{(j)})$ for all mobiles in $(J+1)$ cells is defined as follows:

$$F_{\text{inter}} = \frac{\left[\sum_{j=0}^{J}\sum_{i=1}^{g_j} E(m_i^{(j)})\right]^2}{\left[\left(\sum_{j=0}^{J} g_j\right)\sum_{j=0}^{J}\sum_{i=1}^{g_j} E(m_i^{(j)})^2\right]}.$$

Therefore, intercell fairness measures the global fairness in the average transmission rate per mobile per frame time.

C. Error Control Alternatives Under Variable Rate Transmission

Two different hybrid automatic repeat request (ARQ)-based error control schemes, namely, *Selective-Repeat (SR)* and *Go-Back-m (GBm)*, to be used under variable rate packet data transmission are presented in this paper. In the former, each frame transmitted during a frame time is treated independently so that only the frames transmitted with errors will be retransmitted. Therefore, error recovery in this case is similar to error recovery in the classical selective-repeat ARQ scheme, although this is a bit more complicated due to the variable rate transmission.

The *GBm* scheme assumes a whole frame decoding rather than an individual frame decoding within a frame time. That is, the m frames transmitted during a frame time (with transmission rate r_m) are treated as one single frame of length mM bits. Therefore, when the entire frame is declared to have failed after decoding, all the m frames during that frame time will be retransmitted. This scheme is different from the classical *go-back-N ARQ* scheme since the number of retransmitted frames is determined only by the rate adopted (i.e., the transmission window size is variable in this case rather than fixed).

For illustration, flow diagrams of the proposed error control protocols are depicted in Fig. 1 for transmissions from a single user assuming that the acknowledgment delay is T and that the data rate r_m can be selected from the set $\{r_1, r_2, r_4\}$.

The achieved radio link level throughput (β) under these two error control schemes can be expressed by

$$\beta(n_0, n_1, \ldots, n_\varphi) = \sum_{m=1}^{\varphi} m n_m p_{c,m} \text{ frames/frame time} \quad (8)$$

where n_m denotes the number of users choosing rate r_m ($m = 0,1,\ldots,\varphi$), given that the total number of users transmitting simultaneously during a frame time is n (i.e., $\sum_{m=0}^{\varphi} n_m = n$). Here, the probability of correct reception of a frame $p_{c,m}$ is dependent on the physical layer bit-error rate (BER) performance (i.e., $p_{b,m}$) (and hence on the channel interference and fading conditions) and on the error control protocol employed. Specifically, $p_{c,m}$ would be largely dependent on the dynamically allocated transmission rates among mobiles in the different cells.

The probability of correct reception of a frame $p_{c,m}$ for a user transmitting at rate r_m can be expressed as

$$p_{c,m} = \begin{cases} \sum_{e=0}^{t} \binom{M}{e} p_{b,m}^e (1-p_{b,m})^{M-e}, & \text{for } SR \\ \sum_{e=0}^{t_m} \binom{mM}{e} p_{b,m}^e (1-p_{b,m})^{mM-e}, & \text{for } GBm \end{cases} \quad (9)$$

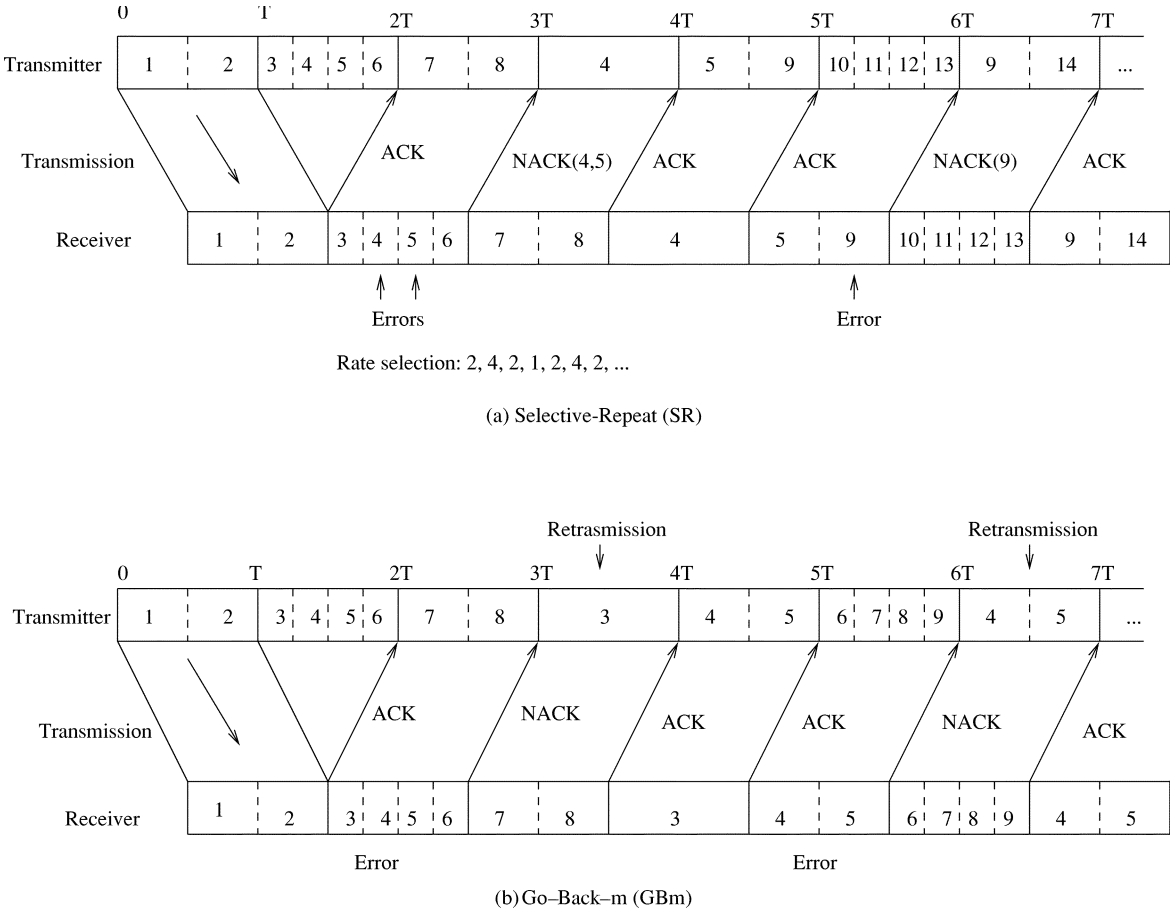

Fig. 1. ARQ-based error control in variable rate transmission systems.

where $p_{b,m}$ is the BER for a user with rate r_m and $\binom{k}{l} \triangleq k!/(k-l)!/l!$. Here, $t(t_m)$-bit error correction capability is assumed for the frame of length $M(mM)$ bits. To make a fair performance comparison between these two error control protocols, the code rates are to be kept the same. For a certain value of t, the *code rate* satisfies the Varsharmov–Gilbert lower bound [12] as given by

$$\text{code rate} \geq 1 - H\left(\frac{d_{\min} - 2}{M}\right) \tag{10}$$

where $H(x) = -x\log_2 x - (1-x)\log_2(1-x)$ and the minimum Hamming distance $d_{\min} \geq 2t+1$. Therefore, for a certain minimum value of *code rate* (corresponding to $d_{\min} = 2t+1$), $d_{\min}$, and hence t_m corresponding to a frame of length mM, can be determined (at least approximately) using (10) with M replaced by mM.

For the *GBm* scheme only the *gross* throughput (in terms of successfully transmitted frames/frame time) is calculated in this paper although the *net* throughput would be lower since the correctly received frames may be retransmitted more than once.

V. Suboptimal Rate Allocation Schemes

In this section, three suboptimal rate allocation procedures, two of which perform the rate allocation on a joint-cell basis, are presented. The performances of these schemes are compared with the performance of the optimal rate allocation scheme in terms of the average transmission rate per mobile per frame time. Note that the avergae transmission rate per mobile can be determined from the sum of the transmission rates as expressed in (7) by dividing it with the total number of mobiles.

A. Peak-Interference-Based Joint-Cell Dynamic Rate Allocation (Algorithm 1)

The idea behind this suboptimal scheme is to minimize the *peak-interference* to other adjacent cells that is caused by any higher rate allocation in one cell. If a mobile located at near the cell boundary transmits at higher rate, it would cause increased interference to adjacent cells, and consequently, would limit the sum of the transmission rates in those cells. Therefore, maximum allowable rates are allocated to the mobiles with the most favorable interference conditions (with respect to the other cells) in terms of the peak-interference factor.

The proposed rate allocation procedure can be described as follows.

1) Find the peak-interference $\hat{\eta}_j(i) \triangleq \max_{j' \neq j}\{\eta_{j/j'}(i)\}$ to adjacent other cells $j' \neq j$ due to the ith mobile in cell j, and repeat this for all $i = 1, \ldots, g_j$ and $j = 0, 1, \ldots, J$.
2) Allocate the maximum possible rate $m_i^{(j)}$ $(0 \leq m_i^{(j)} \leq \varphi)$ to the mobiles logically arranged in an increasing order of the corresponding peak interferences $\{\hat{\eta}_j(i) \,|\, i = 1, \ldots, g_j;\ j = 0, 1, \ldots, J\}$ as far as the

SINR constraint, i.e., $(\mathrm{SINR})_{o,i}^{(j)} \geq (\mathrm{SINR})_o$ is satisfied for all i and j.

Therefore, among all mobiles to which rate allocation is performed, only one has the rate smaller than the maximum allowable rate (i.e., φ) while all the other mobiles are allocated the maximum allowable rate. The rate distribution resulting from this dynamic rate allocation becomes increasingly "extreme" with increasing $(\mathrm{SINR})_o$ and/or increasing other-cell interference factors.

It is required to properly estimate the set of values $\{\hat{\eta}_j(i)\}$ and these may be obtained from the channel measurements performed periodically in case of soft handoff in power-controlled CDMA. Since such a "joint-cell" rate allocation procedure places some burden on the RNC, a proper selection of J is crucial in reducing the network overhead without causing much loss in the sum of the transmission rates, compared to that for the optimal scheme.

B. Sum-Interference-Based Joint-Cell Dynamic Rate Allocation (Algorithm 2)

The idea behind this scheme is to minimize the composite of the other-cell interference in (5), which is the sum of interferences generated by all the mobiles in a cell to the adjacent cells. When mobiles are located near the intersection of three cells, the sum interference caused by any two other cells becomes largest, and, consequently, the sum of the transmission rates over the three cells may decrease significantly. Therefore, in such a case the sum interference can be controlled effectively by allocating low rate (e.g., "rate 0") to these mobiles. In fact, the effect of spatial distribution of the mobiles on the joint-cell dynamic rate allocation may be more effectively taken into account through sum-interference-based dynamic rate allocation.

The "joint-cell" rate allocation in this case allocates the maximum allowable rate to the mobiles with most favorable interference conditions (with respect to the other cells) in terms of the sum-interference factor which is defined by $\eta_j(i) \stackrel{\triangle}{=} \sum_{j' \neq j} \eta_{j/j'}(i)$ for $i = 1, \ldots, g_j$ and $j = 0, 1, \ldots, J$. The rate distribution in this case is similar to that in the peak-interference-based scheme, that is, only one among all the mobiles, to which rate allocation is done, is allocated a transmission rate smaller than the maximum transmission rate while all the other mobiles are allocated the highest rate (i.e., φ).

Note that the sum-interference-based approach is likely to be more sensitive to the estimation errors compared to the peak-interference-based approach. Again, a proper selection of J is also important for the sum-interference-based rate allocation scheme, because this affects not only the network overhead to estimate the sum-interference factors but also the resulting estimation errors. In general, the sensitivity to such estimation errors would be reduced as J decreases, and the network overhead would also become smaller. Therefore, it is necessary to investigate the average transmission rate as a function of J, which would allow us to find a proper value of J to be used in the joint-cell rate allocation.

C. Mean-Sense Approximation-Based Single-Cell Dynamic Rate Allocation (Algorithm 3)

Since the "joint-cell" suboptimal rate allocation schemes require estimation of other-cell interference factors across all $(J + 1)$ cells, the network overhead may become high for large values of J. Therefore, we consider the following simple "single-cell" dynamic rate allocation scheme which does not require estimation of the other-cell interference factors but rather relies on a mean-sense approximation of the other-cell interference. This formulation enables us to map the dynamic rate allocation problem under constrained SINR into the radio link level throughput maximization problem under integrated rate and error control, as will be described later in this paper.

For this scheme we have the following.

1) The composite of the other-cell interference in (5) is approximated in mean sense as follows (see the Appendix):

$$\sum_{j' \neq j} \sum_{k=1}^{g_{j'}} m_k^{(j')} \eta_{j'/j}(k) \longrightarrow \left(\sum_{k=1}^{g_j} m_k^{(j)} \right) \cdot \bar{\eta}_j \qquad (11)$$

where we have assumed $1/J \sum_{j' \neq j} g_{j'} = g_j = G$, i.e., similar traffic load in the "tagged cell" and the other adjacent cells in mean sense and the *average* other-cell interference factor in the tagged cell j is defined by

$$\bar{\eta}_j = \sum_{j' \neq j} \left(\frac{1}{g_{j'}} \sum_{k=1}^{g_{j'}} \eta_{j'/j}(k) \right). \qquad (12)$$

Regarding the computation of $\bar{\eta}_j$, we assume that the mobiles are randomly located in the other cells and the area-average in [13] is chosen to be $\bar{\eta}_j$; therefore, exact estimation of the other-cell interference factors can be avoided. Note that $\bar{\eta}_j$ may vary from frame time to frame time depending on the mobility of the users and the channel-fading conditions.

To model the average other-cell interference factor in tagged cell j in mean sense for unequal traffic distributions, (11) may be modified as follows:

$$\sum_{j' \neq j} \sum_{k=1}^{g_{j'}} m_k^{(j')} \eta_{j'/j}(k) \longrightarrow \left(\sum_{k=1}^{g_j} m_k^{(j)} \right) \cdot \bar{\eta}_j^*$$

where $\bar{\eta}_j^*$ may be well approximated to

$$\bar{\eta}_j^* = \sum_{j' \neq j} \left(\frac{g_{j'}}{g_j} \right) \left(\frac{1}{g_{j'}} \sum_{k=1}^{g_{j'}} \eta_{j'/j}(k) \right).$$

2) With constant (desired) received power level P_b at the tagged $(\mathrm{BS})_j$, the transmit power levels $\{P_{b,i}^{(j)}\}$ (which are inversely proportional to the channel gains $\{\rho_j(j,i) L_j(j,i)\}$) for all mobiles in cell j are used as the channel measurements for dynamic rate allocation among mobiles in cell j.

3) With the *mean-sense* approximation to the other-cell interference, the RAKE-combined output SINR in (5) can be rewritten as

$$(\mathrm{SINR})_{o,i}^{(j)} = \left[\frac{1}{3N} \left(\sum_{k=1}^{g_j} m_k^{(j)} \right) (1 + \bar{\eta}_j) + \left(\frac{2E_b}{N_o} \right)^{-1} \right]^{-1}. \qquad (13)$$

Then, the sum of the transmission rates in cell j can be evaluated by combining (13) with (7), given the parameters $\bar{\eta}_j$ and E_b/N_o.

4) Once the sum of the transmission rates $\sum_{i=1}^{g_j} m_i^{(j)}$ is obtained, the dynamic rate allocation is performed by allocating the maximum allowable rate to the mobiles (logically arranged in an increasing order of the transmit power levels) as far as the sum of the transmission rates is not exceeded.

Note that the transmit power levels account only for the channel gains between the mobiles in the tagged cell j and $(\mathrm{BS})_j$ while the channel gains between the mobiles and other $(\mathrm{BS})_{j'}$ are neglected. In addition, the mean-sense approximation does not fully exploit the spatial distribution of mobiles in other cells. To investigate the effectiveness of mean-sense approximation, the performance of the proposed single-cell dynamic rate allocation scheme is compared to the performances of the joint-cell suboptimal rate allocation schemes.

D. Implementation Issues

To implement the proposed suboptimal rate adaptation schemes, the other-cell interference factors $\{\eta_{j'/j}(k)\}$ in (6) need to be estimated periodically. This can be done within the existing framework for power control and soft handoff in WCDMA networks. During closed-loop power control, each BS measures the uplink received signal strengths from which the in-cell channel gain $\rho_{j'}(j',k)L_{j'}(j',k)$ in (6) can be accurately estimated. Again, to prepare for soft handoff, each mobile station periodically measures the downlink signal strengths from its neighboring BSs. Therefore, this information can be conveyed to the BS through uplink control channel (e.g., DPCCH in ETSI WCDMA [1]) and due to channel reciprocity, the channel gain $\rho_j(j',k)L_j(j',k)$ in (6) can be estimated. Note that, due to the distance-dependent loss [as given in (3)], the contribution of the long-term fading $L_j(j',k)$ is dominant in the channel gain. In this way, the other-cell interference factors $\{\eta_{j'/j}(k)\}$ in (6) can be periodically estimated in the power control and soft handoff framework to realize the suboptimal rate allocation algorithms.

Algorithm 3, which is based on the mean-sense approximation of other-cell interference, is intended to reduce the network overhead resulting from the estimation of the other-cell interference factors. Since due to the mean-sense approximation the rate allocation based on this algorithm can be either aggressive or conservative, while implementing the algorithm the mean-sense interference factor $\bar{\eta}_j$ may need to be tuned periodically. Again, drift in the assigned rate allocation from the desired allocation can be compensated by SINR-based power control.

VI. Integrated Rate and Error Control Under Mean-Sense Approximation-Based Dynamic Rate Adaptation

In this section, we show that the dynamic rate adaptation (using the mean-sense approximation-based suboptimal scheme) under constrained SINR maps into the throughput maximizing rate allocation procedure.

Let us define the *effective traffic load* (or equivalently, the sum of the transmission rates) x by

$$x \triangleq \sum_{m=1}^{\varphi} m n_m \tag{14}$$

where $\sum_{m=0}^{\varphi} n_m = n = G$ for the single-cell dynamic rate allocation and the rate distribution is simply given by $n_\varphi = \lfloor x/\varphi \rfloor$ and $n_m = 1$ for $m = x - \varphi n_\varphi$ ($\lfloor x \rfloor$ denotes the greatest integer not exceeding x).

Then, given that the other-cell interference and the noise are fixed, the RAKE-combined output SINR in (13) can be expressed as a function of x only, namely,

$$(\mathrm{SINR})_{o,i}^{(j)} = \left[\frac{x(1+\bar{\eta}_j)}{3N} + \left(\frac{2E_b}{N_o} \right)^{-1} \right]^{-1} \triangleq 2\gamma \tag{15}$$

for $\gamma = E_b/N_{o,eq}$ ($N_{o,eq}$ denotes the power spectral density of the equivalent noise).

To determine the radio link level throughput β using (8), we need to calculate $p_{c,m}$ and hence $p_{b,m}$, the BER. To calculate BER, we consider two multipath channel models-multipath Rayleigh fading channel with *equal* average path power and multipath Rayleigh fading channel with *unequal* average path power.[5]

In the case of L-path Rayleigh fading with uncorrelated scattering and equal average path power, since $\sum_{l=1}^{L} \gamma_l = \gamma$ [where γ is as defined in (15)], the effective per-path SINR becomes $\gamma_l = \gamma/L$. For maximal-ratio combining (MRC) with independent L branches, the BER is given by [14]

$$p_b = \left[\frac{1}{2}(1-\zeta) \right]^L \sum_{l=0}^{L-1} \binom{L-1+l}{l} \left[\frac{1}{2}(1+\zeta) \right]^l \tag{16}$$

where $\zeta = \sqrt{\gamma_l/(1+\gamma_l)}$.

In the case of multipath Rayleigh fading with unequal average path power, the effective lth path SINR is $\gamma_l = \sigma_l^2 \gamma$, where $\sigma_l^2 = \mathbf{E}\{a_{j,i(j),l}^2\}$ ($\mathbf{E}$ denotes the expectation) and $\sum_{l=1}^{L} \sigma_l^2 = 1$ (normalized). Then, the BER can be expressed by [14]

$$p_b = \frac{1}{2} \sum_{l=1}^{L} \pi_l \left[1 - \sqrt{\frac{\gamma_l}{1+\gamma_l}} \right] \tag{17}$$

where $\pi_l = \prod_{\substack{l'=1 \\ l' \neq l}}^{L} \gamma_l/(\gamma_l - \gamma_{l'})$.

Note that the BER is a function of only the effective traffic load x and does not depend on the distribution of rate allocations. That is, for the mean-sense approximation-based single-cell dynamic rate allocation procedure, $p_{b,m}$ in (9) is equal to p_b. Therefore, for *SR*-based error control $p_{c,m}$ would be equal to p_c (which is a function of x) while for *GBm*-based error control

$$p_{c,m} = \begin{cases} p_{c,\varphi}, & \text{for } n_\varphi \text{ mobile station(s)} \\ p_{c,x-\varphi n_\varphi}, & \text{for 1 mobile station} \end{cases} \tag{18}$$

[5]Here, the in-cell power control may compensate the multipath fading $\rho_j(j,i)$ from slot to slot during a frame time, where one frame time is typically divided into 16 power control slots (as in ETSI WCDMA [1]), but the instantaneous fluctuations in the signal amplitude level during a bit time are assumed to follow these channel models.

with $n_\varphi = \lfloor x/\varphi \rfloor$. Therefore, throughput β in (8) can be rewritten as

$$\beta(n_0, n_1, \ldots, n_\varphi) = \begin{cases} x \cdot p_c, & \text{for } SR \\ \varphi n_\varphi \cdot p_{c,\varphi} + (x - \varphi n_\varphi) \cdot p_{c,x-\varphi n_\varphi}, & \text{for } GBm. \end{cases} \quad (19)$$

Since p_c (as well as $p_{c,\varphi}$, $p_{c,x-\varphi n_\varphi}$) decreases as x increases (and vice versa) for both the error control protocols, the throughput can be optimized when x is properly chosen. Since under certain channel fading and interference conditions the sum of the transmission rates x depends on the target SINR (i.e., $(\mathrm{SINR})_o$), for a given error control protocol (e.g., *SR* or *GBm*) the target SINR can be controlled such that the peak throughput is achieved. Again, under a given error control protocol, for a certain target SINR, the forward error correction (FEC) parameter t can be adjusted such that the total radio link level *throughput* is maximized. In this way, the single-cell dynamic rate allocation under constrained SINR in the presence of other-cell interference and noise reduces to the throughput-maximizing rate allocation problem and the rate control can be integrated with error control to maximize the radio link level throughput.

VII. Simulation Model, Results, and Discussions

A. Models for Micromobility, Shadowing, and Multipath Fading

We consider two micromobility models: the *random mobility* model and the *directional mobility* model. In the former case, the location of each mobile user during each frame time is chosen randomly inside the target cell and the effect of shadowing at the different mobile locations is assumed to be uncorrelated. In the latter case, we assume a directional random walk model [15] where the mobile users travel from a starting point to a destination in a series of statistically independent discrete steps, and in this case the effect of shadowing at the different locations is assumed to be correlated. For each step, the angular deviation (θ) of the travel direction from the *principal direction*[6] has the probability density function $f(\theta)$ given by

$$f(\theta) = \begin{cases} \frac{A_\theta}{2[1+A_\theta^2\theta^2]\tan^{-1}(A_\theta\pi)}, & -\pi \le \theta \le \pi \\ 0, & \text{otherwise.} \end{cases} \quad (20)$$

The parameter A_θ controls how close the travel direction is to the principal direction. If a mobile user travels in a forward direction with probability 0.95, the corresponding value for A_θ is 4.2 [15]. We assume that all the mobile users have a constant speed of v and that for each user the successive points are separated (in time) by one frame time.

The correlated shadowing is modeled as a Gaussian white noise process, filtered through a first degree low-pass filter as follows [16]:

$$\omega_{k+1(\mathrm{dB})} = a \times \omega_{k(\mathrm{dB})} + (1-a) \times u_k \quad (21)$$

where $\omega_{k(\mathrm{dB})}$ is the mean envelope level or mean square-envelope level (in decibels) that is experienced at location k, a is the correlation coefficient given by $a = \varepsilon_D^{vT_s/D}$, and u_k is a zero-mean Gaussian random variable with variance $\tilde{\sigma}^2$.

Here, $\tilde{\sigma}^2 = [(1+a)/(1-a)]\sigma^2$ with σ^2 being the variance of log-normal shadowing. The parameter ε_D is the correlation between two points separated by distance D and T_s is the sampling interval (which is assumed to be equal to the frame time T in this paper).

Multipath fading is assumed to be independently varying. In the random mobility case, an L-path ($L = 3$) Rayleigh fading channel with uncorrelated scattering and equal average path power is considered. Multipath fading with unequal average path power is considered for the directional mobility with correlated shadowing case and the parameters are based on the vehicular-B model [17] for macrocell.

[6]At any point on the travel path, the line joining the point to the destination defines the principal direction.

TABLE II
Simulation Parameters

Parameter	Value
Frame time, T	10 ms
Chip sequence length, N	128
Path-loss exponent, δ	4.0
Standard deviation of shadow fading, σ	8 dB
ν	0.2
σ_{err}	-1.0, -5.0, -10.0, -15.0 dB
D	100 m
ε_D	0.1
A_θ	4.2
v	20, 50, 80 km/hr
φ	8
J	2, 6, 18
FEC parameter, t	1, 2, 3, 4
L	3

B. Modeling Estimation Error

The estimation error is modeled as multiplicative noise. The estimation error η_{err} corresponding to each of the other-cell interference factors $\eta_{j'/j}(k)$ is generated as a log-normal random variate with standard deviation $\sqrt{2}\sigma_{\mathrm{err}}$. Therefore, the estimated other-cell interference factors are calculated as follows:

$$\eta_{j'/j}^{(est)}(k) = \eta_{j'/j}(k) \times \eta_{\mathrm{err}}. \quad (22)$$

C. Simulation Methodology

For the random mobility with uncorrelated shadowing case, the locations of the mobiles in the target cell are generated randomly during each iteration and the number of iterations used for collecting the results is sufficiently large (e.g., 10^5). In the case of directional mobility model with correlated shadowing, during each iteration the initial locations of the mobiles are generated randomly within the target cell and the successive locations are generated by using (20) based on the mobile speed (v) and the length of the adaptation interval (or measurement interval or frame time T). The destination point is assumed to be located in the target cell and while generating the successive mobile locations it is ensured that the locations are within the target cell.

It is to be noted that the correlation between shadowing in the two successive locations is affected by the mobile speed

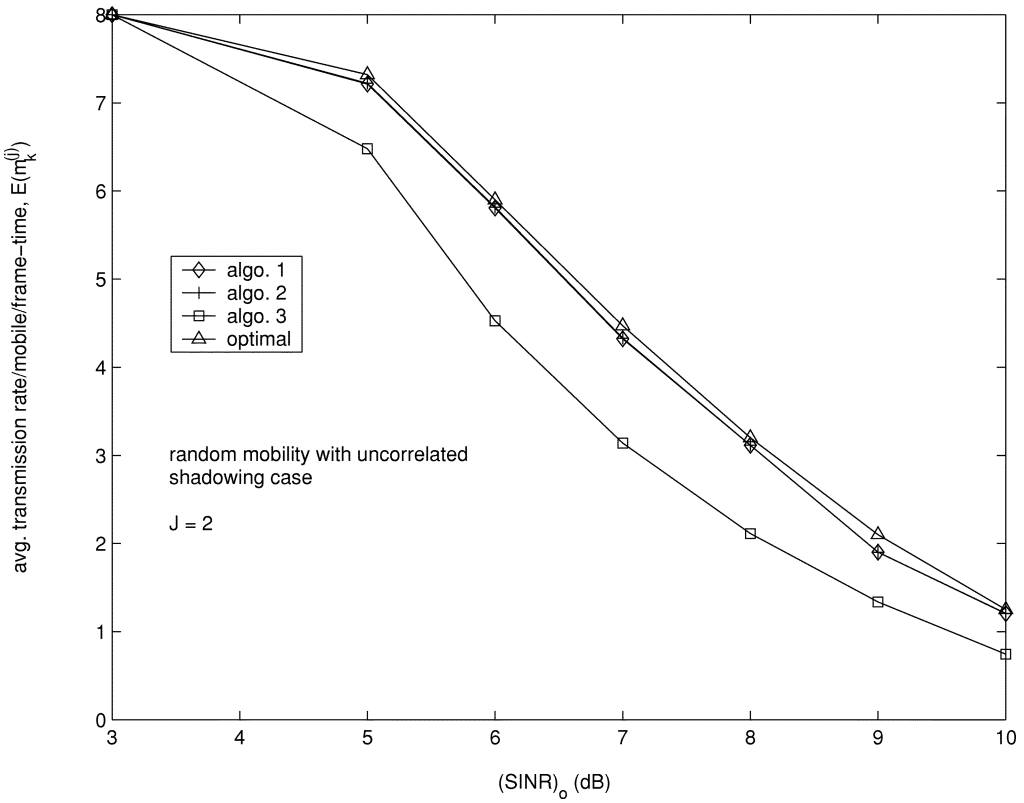

Fig. 2. Performance comparison among the optimal and the suboptimal rate allocation schemes.

and the measurement interval. The total number of iterations for each mobile during each simulation is taken to be sufficiently large (e.g., 10^5) to ensure reliability of the obtained performance measures.

In each case, simulations are performed to obtain the maximum average value of the transmission rate per mobile.[7] In this case, $L_{j'}(j',k) > L_j(j',k)$, $\forall j' \neq j$. The values of $L_{j'}(j',k)$ and $L_j(j',k)$, which account for the long-term fading, are assumed to be constant over a frame time T.

The values of $\rho_j(j',k)$ and $\rho_{j'}(j',k)$, which account for the short-term fading in (6), are assumed to be constant only over a fraction of the frame time Δt, where $T = K\Delta t$. Therefore, the value of $\eta_{j'/j}(k)$ over a frame time is calculated by using the average of the K independent values of $\rho_j(j',k)/\rho_{j'}(j',k)$. The value of K is assumed to be 16 in this paper.

To investigate the sensitivity of the *peak-interference-based* and the *sum-interference-based* rate allocation algorithms to the estimation errors, the other-cell interference factors $\eta_{j'/j}^{(est)}(k)$ in (22) are used to determine the rate allocations $m_k^{(j')}$, where higher rates are allocated to the mobiles with least peak/sum-interference factors, while the SINR constraint in (7) is tested using the true values $\eta_{j'/j}(k)$, instead of $\eta_{j'/j}^{(est)}(k)$.

In the case of mean-sense approximation-based rate allocation, the values of $\bar{\eta}_j$ (for $j = 0, 1, \ldots, J$) are generated during each frame time depending on the location of the mobiles in the other J cells (with $g_{j'} = g_j = 10, \forall j' \neq j$). Rate allocation in each cell is based on the above calculated $\bar{\eta}_j$. The average transmission rate per mobile per frame time is obtained over all the cells over the simulation period. In fact, the area-average other-cell interference factor is rather optimistic; therefore, if we allocate rates in a given cell based on the area-average interference, the average transmission rate per mobile per frame time in that tagged cell may become higher than the average transmission rate per mobile per frame time over all the cells. Therefore, for performance comparison with the peak-interference and the sum-interference based-schemes, we evaluate the average transmission rate per mobile per frame time over all the cells for this scheme.

Since due to the spatial distribution of the mobiles and the random nature of the channel shadowing and fading conditions the other-cell interference factors vary from frame time to frame time, for a fair comparison among the performances of the optimal rate allocation with the performances of the suboptimal rate allocation schemes, the average transmission rate per mobile per frame time is evaluated for all the schemes under similar statistical variations of the other-cell interference factors.

The values of some of the system parameters used for obtaining the results presented in this paper are listed in Table II. We consider a nonuniform traffic scenario in $(J+1)$ cells ($J =$ 2, 6, 18) with $\{g_0, g_1, g_2, \ldots, g_J\} = \{8, 10, 12, 8, \ldots\}$ for the joint-cell suboptimal rate allocation schemes. Note that $J = 18$ corresponds to a three-tier cell layout [18]. The average transmission rate per mobile per frame time ($E(m_k^{(j)})$) is calculated based on the average transmission rate per mobile per frame time corresponding to each mobile in each of these $(J+1)$ cells. For the single-cell rate allocation we assume $g_0 = g_1 = g_2 = \cdots = g_J = G = 10$.

[7]The average transmission rate per mobile may fall below this maximum value in the case of soft handoff due to increased $\eta_{j'/j}(k)$.

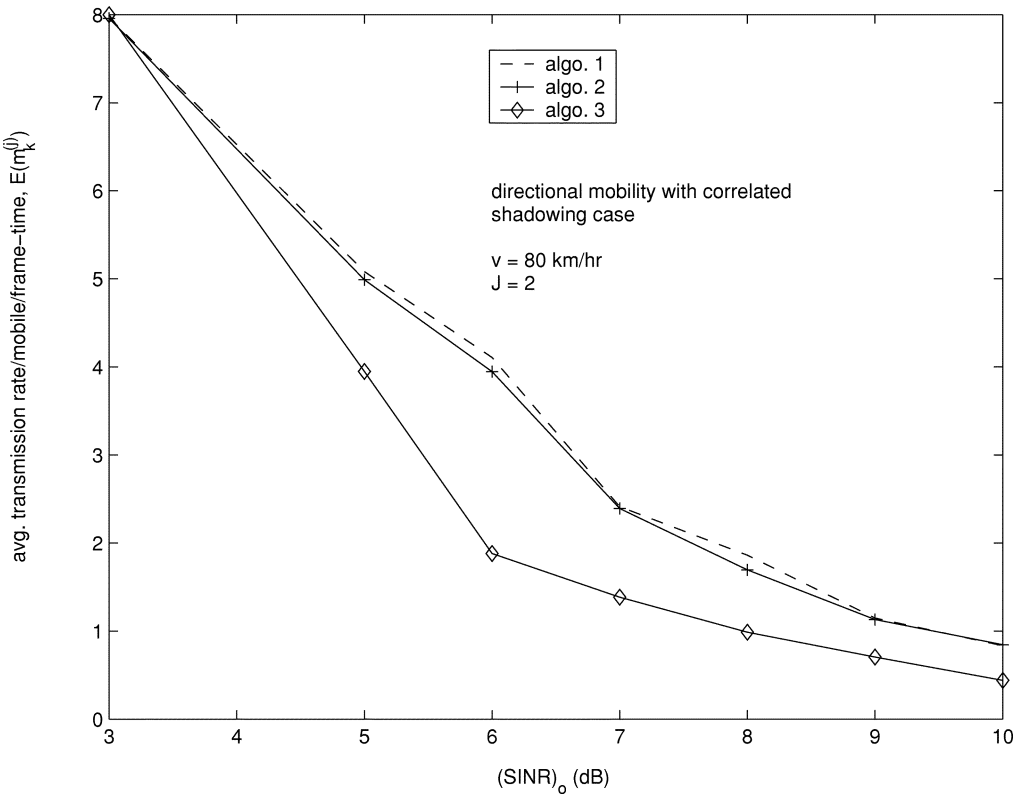

Fig. 3. Performance comparison among the suboptimal rate allocation schemes for the directional mobility with correlated shadowing case.

D. Performance Results and Discussions

1) Comparative Performance With Respect to Average Transmission Rate per Mobile per Frame Time: Typical variations in the average transmission rate per mobile per frame time $E(m_k^{(j)})$ with the desired signal-to-interference-plus-noise ratio $(\mathrm{SINR})_o$ are demonstrated in Fig. 2 for dynamic rate adaptation using the optimal algorithm and the three other schemes described above. Interestingly, both the peak-interference-based and the sum-interference-based dynamic rate allocation schemes are observed to perform no worse than the optimal dynamic rate allocation, which is determined by an exhaustive search over all possible combinations of rate allocations among all the mobiles in all the cells under given SINR constraint. This phenomenon can be attributed to the fact that both the peak-interference-based and the sum-interference-based dynamic rate allocation schemes tend to reduce the other-cell interference (by allocating lower rates to mobiles located presumably near the boundary of the cells) in order to increase the average transmission rate. In fact, the "greedy" approaches of the peak-interference and the sum-interference-based rate allocation make the average transmission rate achieved for these two cases very close to that for the optimal scheme.

For both the micromobility models-random mobility with uncorrelated shadowing and directional mobility with correlated shadowing, the performance difference between the peak-interference-based and the sum-interference-based rate allocation schemes is not significant (Figs. 2 and 3). For the mean-sense approximation-based dynamic rate allocation, the average transmission rate is observed to be smaller compared to the two other schemes. This is due to the fact that the mean-sense approximation overestimates the other-cell interference factor compared to the actual values. Therefore, the joint-cell rate allocation schemes can better exploit the spatial distribution of all mobiles over all the cells compared to the mean-sense approximation-based scheme.

2) Fairness in Achieved Average Transmission Rate per Mobile: Under the proposed dynamic rate adaptation schemes, the intercell fairness (F_{inter}) in average transmission rate is largely affected by the user mobility patterns (and hence the spatial distribution of the users) and the target SINR (i.e., $(\mathrm{SINR})_o$). Typical variations in F_{inter} for the three rate allocation schemes are illustrated in Fig. 4 for both the micromobility models.

For all the three schemes, the fairness deteriorates for the directional mobility with correlated shadowing case compared to that for the random mobility with uncorrelated shadowing case. This is presumably due to the fact that, under the directional mobility model, the users moving near/along the boundary of a cell would be allocated lower transmission rates compared to those located nearer to the BS. In the random mobility case, at the beginning of each frame time all the mobiles are assumed to be randomly located inside the cells, and, therefore, the possibility of a mobile being allocated lower/higher transmission rate during successive frame times is reduced. This, in turn, reduces unfairness in the achieved average transmission rate per mobile per frame time over a finite time interval.

Since with increased $(\mathrm{SINR})_o$ the rate distribution resulting from the dynamic rate allocation becomes more extreme (i.e.,

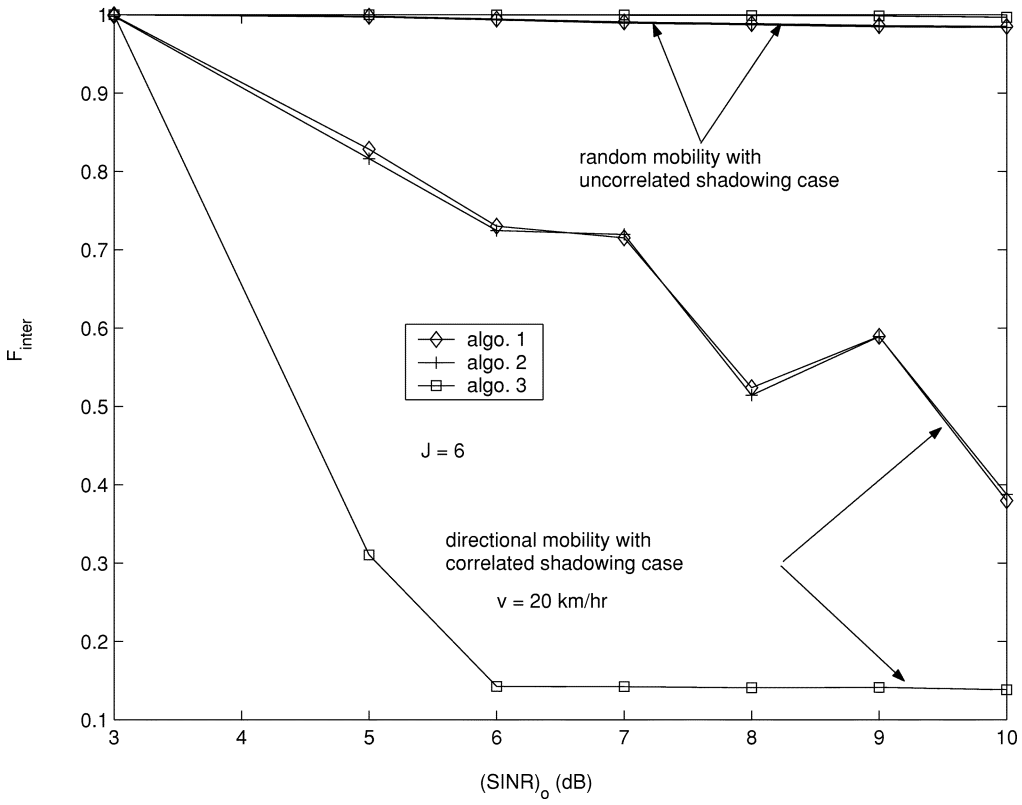

Fig. 4. Fairness in the achieved average transmission rate per mobile per frame time.

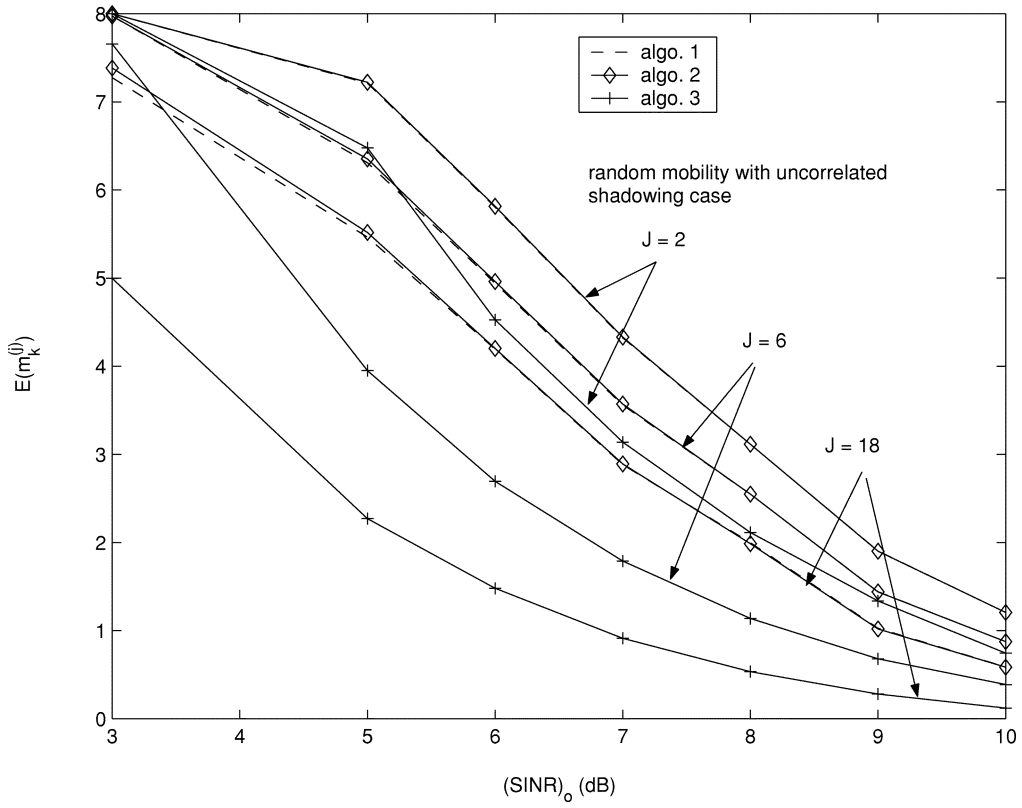

Fig. 5. Impact of J on the average transmission rate per mobile per frame time.

fewer number of mobiles are allocated the maximum possible rate while the other mobiles are allocated "rate 0"), the fairness deteriorates with increasing $(\mathrm{SINR})_o$.

3) Selection of J: Sensitivity of the average transmission rate to variations in the parameter J is illustrated in Fig. 5. As is evident from Fig. 5, the average transmission rate monotoni-

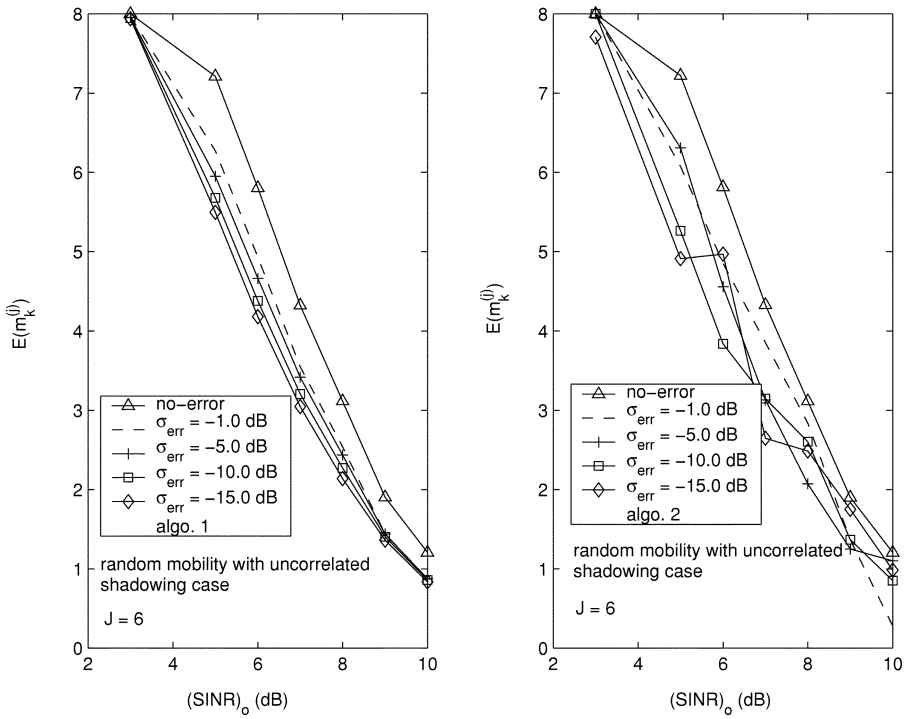

Fig. 6. Sensitivity of average transmission rate to variations in estimation errors for the random mobility with uncorrelated shadowing case.

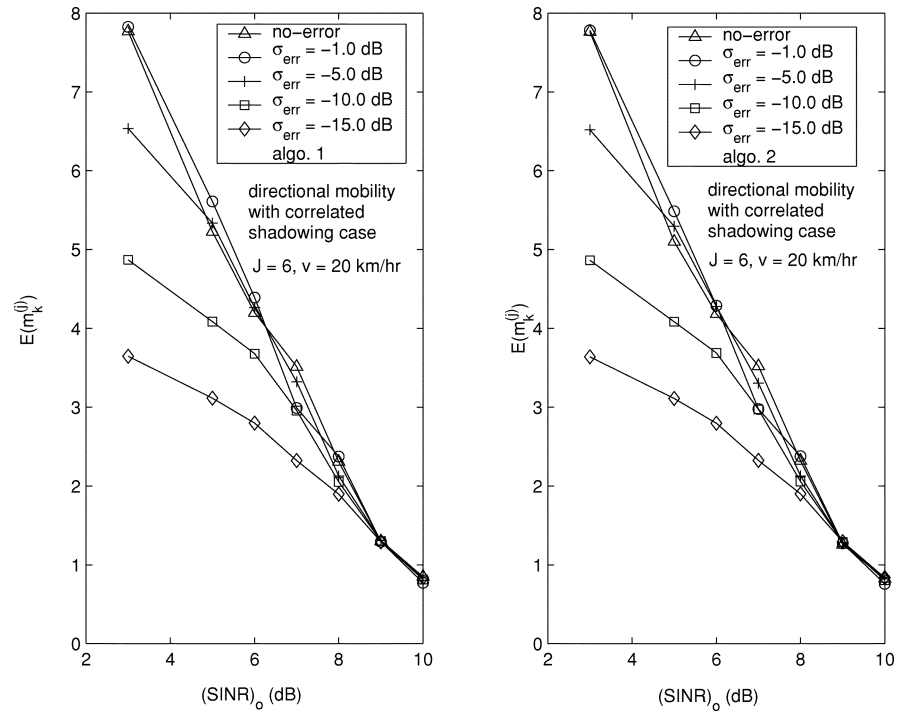

Fig. 7. Sensitivity of average transmission rate to variations in estimation errors for the directional mobility with correlated shadowing case.

cally decreases with increasing J. Since the larger the value of J is, the greater is the deviation of average other-cell interference factor from the actual values, the impact of increasing J on the achieved average transmission rate becomes more pronounced for the mean-sense approximation-based dynamic rate allocation.

Since the network overhead due to estimation of the other-cell interference factors may become significant for large J, the choice of J for "joint-cell" rate allocation would be based on the desired/permissible network overhead.

4) Impact of Estimation Error: For the peak-interference-based and the sum-interference-based rate allocation, the other-cell interference factor corresponding to a mobile in a cell and the rate allocation corresponding to that mobile contribute to the interference in the other cells. Therefore, errors in the estimation of the other-cell interference factors impact the

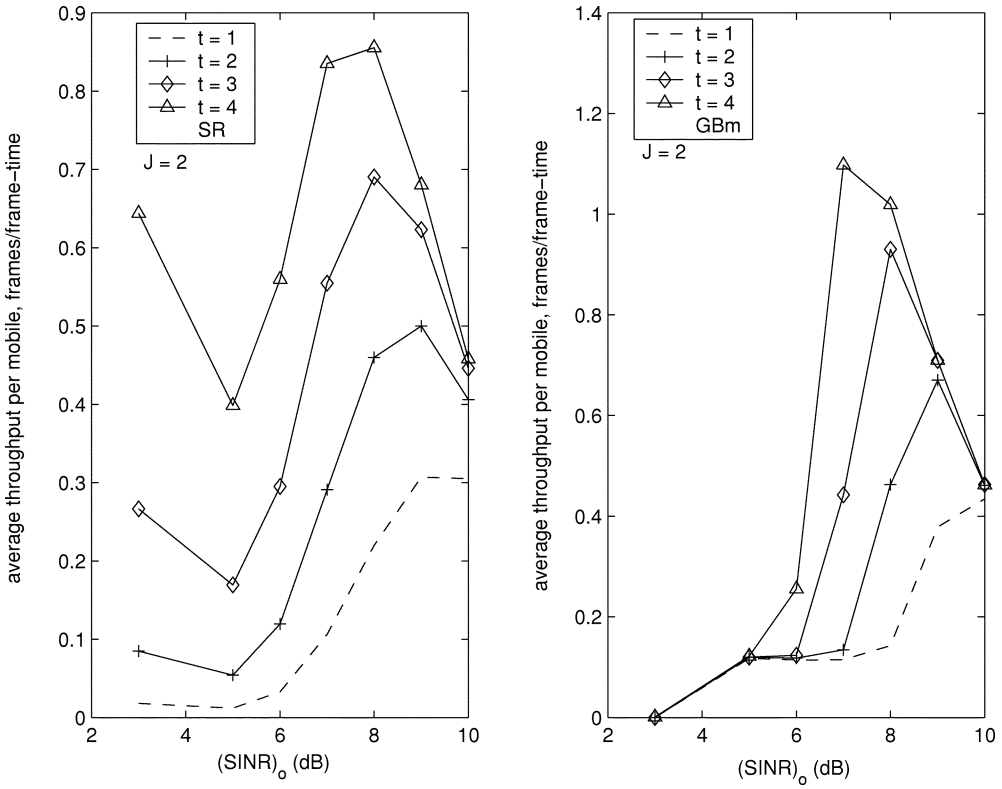

Fig. 8. Impact of FEC parameter on the radio link level throughput (for *SR* and *GBm*-based error control and *mean-sense approximation*-based dynamic rate allocation).

rate allocation in other cells and hence the achieved average transmission rate by each mobile.

The impact of estimation errors on the average transmission rate for the random and directional mobility models are illustrated in Figs. 6 and 7. The achieved average transmission rate per mobile depends on the estimation-error variance ($\sigma^2_{\rm err}$) and the loss in the average transmission rate can be significant when the desired signal-to-noise-plus-interference ratio $(\mathrm{SINR})_o$ is relatively small (Fig. 7). For small $(\mathrm{SINR})_o$, presumably a larger number of mobiles are allocated the largest possible rate, and, consequently, the impact of the other-cell interference (as manifested in $\eta_{j'/j}(k) \times m_k^{(j')}$) on the achieved $(\mathrm{SINR})_{o,i}^{(j)}$ becomes more pronounced. Therefore, estimation errors in other-cell interference significantly deteriorate the average transmission rate. Note that since the noise due to estimation error is assumed to be multiplicative, the accuracy in the estimation of other-cell interference decreases with decreasing $\sigma_{\rm err}$ (in decibels).

Since for the sum-interference-based rate allocation scheme the estimation errors are accumulated in the "sum interference," the impact of estimation errors on rate allocation corresponding to mobiles in a cell would become more pronounced with increasing J. This, in turn, impacts the rate allocation in other cells and ultimately the achieved average transmission rate per mobile per frame time. Specifically, with increasing J, the estimation errors in other-cell interference factors corresponding to the mobiles in a cell would more significantly impact the rate allocation in the adjacent cells in the case of sum-interference-based rate allocation.

5) Integrated Rate and Error Control: Under the mean-sense approximation-based single-cell dynamic rate adaptation, the radio link level throughput (β) can be maximized with a proper choice of the target SINR (i.e., $(\mathrm{SINR})_o$) and the radio link level error control mechanism. For both the error control schemes described in this paper, dynamic rate allocation with SINR constraint can be used to determine the throughput-maximizing rate allocation that produces the maximum radio link level throughput under different traffic load.

Typical variations in the average radio link level throughput per mobile β with $(\mathrm{SINR})_o$ for both the *SR* and the *GBm*-based error control are illustrated in Fig. 8 for different values of the FEC parameter t for the random mobility with uncorrelated shadowing case. Similar results are obtained for the directional mobility case. The impact of variations in the average traffic load G on throughput β is illustrated in Fig. 9.

Under certain traffic load and channel condition, for both the *SR* and the *GBm* error control protocols, β is effectively a function of $(\mathrm{SINR})_o$. For lower values of $(\mathrm{SINR})_o$, although the average transmission rate allocated per mobile is higher, the frame-error rate is also significantly higher especially when the value of the FEC parameter (t) is small (i.e., code rates are larger); consequently, the average throughput is reduced. Again, too much "conservativeness" in terms of the target SINR and, hence, radio link level reliability may deteriorate the achieved throughput performance due to the reduced average transmission rate per frame time.

Since the average transmission rate per mobile per frame time decreases with increasing average traffic load (G), the radio link level throughput per mobile (β) diminishes as G increases. With dynamic rate adaptation under constrained SINR, β can be maximized with a proper choice of the target SINR (Fig. 9). Under similar conditions, the radio link level throughput is better with

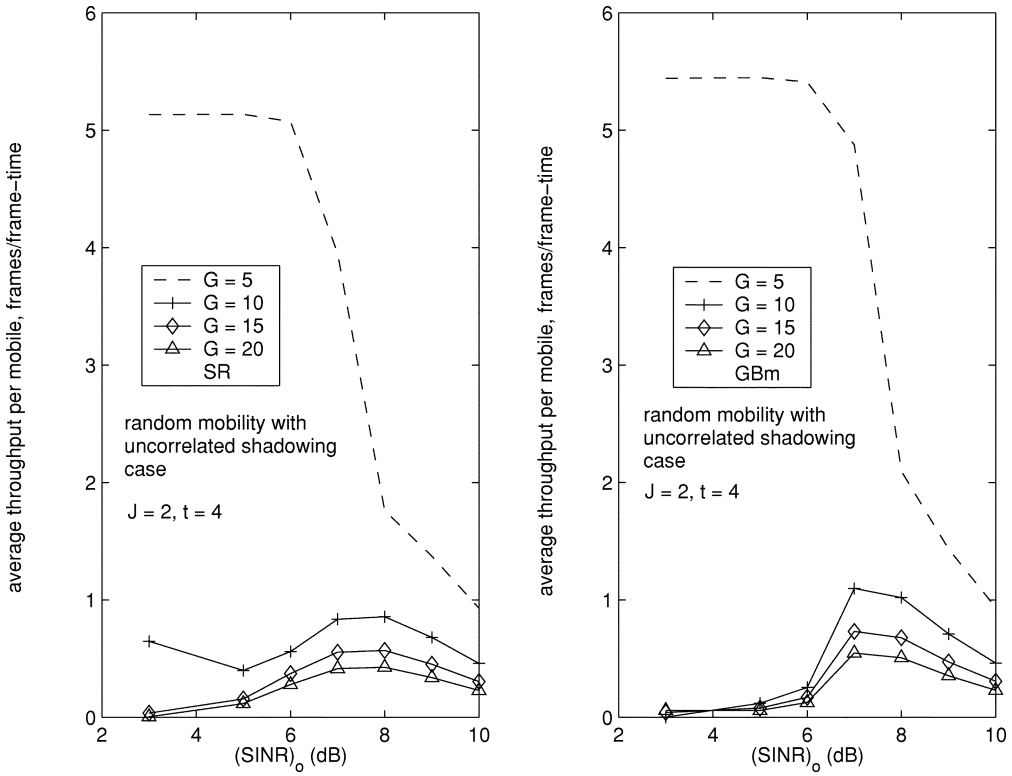

Fig. 9. Radio link level throughput under different average traffic load (for *SR* and *GBm*-based error control and *mean-sense approximation*-based dynamic rate allocation).

the *GBm* error control protocol compared to that with the *SR* error control protcol. However, as mentioned before, the *net* throughput (or goodput) for the *GBm* case would be smaller than those shown in Figs. 8 and 9. Again, the choice of the proper radio link level protocol between these two would be determined based on the implementation complexity of these schemes.

VIII. Conclusion

Based on a general SINR model for uplink variable rate transmission in cellular WCDMA networks, the problem of optimal dynamic rate adaptation under constrained SINR has been formulated considering a single class of users. Three different interference-based dynamic rate adaptation algorithms with reduced computational complexity have been introduced. Two different error control alternatives in a variable rate packet data transmission scenario have been presented and their performances have been analyzed for the mean-sense approximation-based dynamic rate adaptation. It has been shown that the problem of dynamic rate adaptation under constrained SINR maps into the problem of radio link level throughput maximization under integrated rate and error control. Performance evaluation for the proposed schemes has been carried out for the random mobility with uncorrelated shadowing and the directional mobility with correlated shadowing cases.

The following provides a summary of the key results.

1) Optimal dynamic rate allocation (which could be found through exhaustive search) provides no better average transmission rate per mobile than the proposed suboptimal heuristic-based dynamic rate allocation schemes. The mean-sense approximation-based approach provides a rather conservative estimate of the average transmission rate compared to the peak-interference and the sum-interference-based approaches.
2) Directional mobility and correlated shadowing reduces the fairness in average transmission rates among the mobiles in the different cells compared to the random mobility with uncorrelated shadowing case.
3) The average transmission rate per mobile per frame time deteriorates with increasing J, and, hence, the number of cells being considered for "joint-cell" rate allocation. This is particularly significant for the mean-sense approximation-based dynamic rate allocation.
4) Estimation errors adversely affect the transmission rate per mobile per frame time, especially for the directional mobility with correlated shadowing case when the target SINR is small. The average transmission rate per mobile per frame time for the sum-interference-based rate allocation scheme is more sensitive to the estimation errors and the parameter J.

The proposed model for performance evaluation under dynamic radio link level rate adaptation would be used in our future work to evaluate the performance of transmission control protocol (TCP) in wide area cellular WCDMA networks. In addition, the problem of dynamic rate adaptation in cellular multirate WCDMA networks under multiple level of QoS constraints will be also addressed.

Appendix
Evaluation of the Other-Cell Interference in (11)

Suppose that a cell is loaded with the effective traffic load x_j $(j = 0, 1, \ldots)$ as given in (14), where x_0 is associated with tagged center cell 0 and $\{x_j\}$ $(j \geq 1)$ with other neighboring

cells. In cellular power controlled-CDMA [13], the other-cell interference is affected by Rayleigh multipath fading, path loss, and shadowing, modeled as a multiplicative loss of η_j, which yields the composite of the other-cell interference as $\eta_1 x_1 + \eta_2 x_2 + \cdots$. Due to the law of large numbers, it fairly approaches an expectation, namely, $\mathbf{E}\{\eta_1 x_1 + \eta_2 x_2 + \cdots\}$, which is

$$\mathbf{E}\{\eta_1 x_1 + \eta_2 x_2 + \cdots\} \longrightarrow \bar{\eta}_j \cdot \mathbf{E}\{x\} \tag{23}$$

with $\bar{\eta}_j$ as defined in (12). Since we are assuming equal traffic load in mean sense ($1/J \sum_{j=1}^{J} g_j = g_0 = G$), $\mathbf{E}\{x\}$ is well approximated by x as given in (14) with $n = G$, and the average other-cell interference factor $\bar{\eta}_j$ is calculated by the area-average of $\sum_{j \geq 1} \eta_j$ in [13].

REFERENCES

[1] E. Dahlman *et al.*, "UMTS/IMT-2000 based on wideband CDMA," *IEEE Commun. Mag.*, vol. 36, pp. 70–80, Sept. 1998.

[2] E. Dahlman and K. Jamal, "Wide-band services in a DS-CDMA based FPLMTS system," *Proc. IEEE VTC '96*, pp. 1656–1660.

[3] S. Nanda, K. Balachandran, and S. Kumar, "Adaptation techniques in wireless packet data services," *IEEE Commun. Mag.*, pp. 54–64, Jan. 2000.

[4] O. Sallent and R. Augustí, "A proposal for an adaptive S-Aloha access system for a mobile CDMA environment," *IEEE Trans. Vehic. Technol.*, vol. 47, pp. 977–985, Aug. 1998.

[5] C.-L I and K. K. Sabnani, "Variable spreading gain with adaptive control for true packet switching wireless network," *Proc. IEEE ICC '95*, pp. 725–730.

[6] S.-J. Oh and K. M. Wasserman, "Dynamic spreading gain control in multiservice CDMA networks," *IEEE J. Select. Areas Commun.*, vol. 7, pp. 918–927, May 1999.

[7] S. Ramakrishna and J. M. Holtzman, "A scheme for throughput maximization in a dual-class CDMA system," *IEEE J. Select. Areas Commun.*, vol. 16, pp. 830–844, Aug. 1998.

[8] A. D. Wyner, "Shanon-theoretic approach to a Gaussian cellular multiple access channel," *IEEE Trans. Inform. Theory*, vol. 44, pp. 1713–1727, Nov. 1994.

[9] S. Ulukus and L. J. Greenstein, "Throughput maximization in CDMA uplinks using adaptive spreading and power control," *Proc. IEEE ISSSTA '00*, pp. 565–569, Sept. 2000.

[10] M. B. Pursley, "Performance evaluation for phase-coded spread-spectrum multiple-access communication—Part I: System analysis," *IEEE Trans. Commun.*, vol. 25, pp. 795–799, Aug. 1977.

[11] V. A. Alfred and D. U. Jeffrey, *Foundations of Computer Science (C Edition)*: Computer Sci. Press, 1998.

[12] W. W. Peterson and E. J. Weldon, *Error Correcting Codes*. Cambridge, MA: M.I.T. Press, 1972.

[13] A. J. Viterbi, A. M. Viterbi, and E. Zehavi, "Other-cell interference in cellular power-controlled CDMA," *IEEE Trans. Commun.*, vol. 42, pp. 1501–1504, Feb./Mar./Apr. 1994.

[14] J. G. Proakis, *Digital Communications*, 2 ed. New York: McGraw-Hill, 1989.

[15] T. K. Kim and C. Leung, "Generalized paging schemes for cellular communications systems," *Proc. IEEE PACRIM '99*, pp. 217–220.

[16] M. Gudmundson, "Correlation model for shadow fading in mobile radio systems," *IEE Electron. Lett.*, vol. 27, no. 23, pp. 2145–2146.

[17] "Guidelines for Evaluation of Radio Transmission Technologies for IMT-2000,", Rec. ITU-R M.1225, 1997.

[18] K. S. Gilhousen *et al.*, "On the capacity of a cellular CDMA system," *IEEE Trans. Vehic. Technol.*, vol. 4, pp. 303–312, May 1991.

Dong In Kim (S'89-M'91-SM'02) received the B.S. and M.S. degrees in electronics engineering from Seoul National University, Seoul, Korea, in 1980 and 1984, respectively, and the M.S. and Ph.D. degrees in electrical engineering from University of Southern California (USC), Los Angeles, in 1987 and 1990, respectively.

From 1984 to 1985, he was with the Korea Telecom Research Center as a Researcher. From 1986 to 1988, he was a Korean Government Graduate Fellow in the Department of Electrical Engineering, USC. In 1991, he was with the University of Seoul, Seoul, Korea, leading the Wireless Communications Research Group. He is now with Simon Fraser University, Burnaby, Canada, where he is an Associate Professor of the School of Engineering Science. He was a Visiting Professor at University of Victoria, Victoria, Canada, from 1999 to 2000. He has performed research in the areas of packet radio networks and spread-spectrum systems since 1988. His current research interests include spread-spectrum systems, cellular mobile communications, indoor wireless communications, and wireless multimedia networks.

Dr. Kim has served as an Editor for the IEEE JOURNAL ON SELECTED AREAS IN COMMUNICATIONS: Wireless Communications Series and also as a Division Editor for the *Journal of Communications and Networks*. Currently, he serves as an Editor for the IEEE TRANSACTIONS ON COMMUNICATIONS and the IEEE TRANSACTIONS ON WIRELESS COMMUNICATIONS.

Ekram Hossain (S'98-M'01) received the B.Sc. and M.Sc. degrees, both in computer science and engineering, from Bangladesh University of Engineering and Technology (BUET), Dhaka, Bangladesh, in 1995 and 1997, respectively. He received the Ph.D. degree in electrical engineering from University of Victoria, Victoria, Canada, in 2000.

He is an Assistant Professor in the Department of Electrical and Computer Engineering at University of Manitoba, Winnipeg, Canada. He was a University of Victoria Fellow. His research interests include radio link control and transport layer protocol design issues for the next-generation wireless data networks.

Dr. Hossain currently serves as an Editor for the IEEE TRANSACTIONS ON WIRELESS COMMUNICATIONS.

Vijay K. Bhargava (S'70–M'74–SM'82–F'92) received the B.Sc., M.Sc., and Ph.D. degrees from Queen's University, Kingston, Canada, in 1970, 1972, and 1974, respectively.

Currently, he is a Professor and Chair of Electrical and Computer Engineering at the University of British Columbia, Vancouver, BC, Canada. He is a co-author of the book *Digital Communications by Satellite* (New York: Wiley, 1981) and co-editor of the book *Reed-Solomon Codes and Their Applications* (New York: IEEE). His research interests include multimedia wireless communications.

Dr. Bhargava is a Fellow of the B.C. Advanced Systems Institute, Engineering Institute of Canada (EIC), the Canadian Academy of Engineering, and the Royal Society of Canada. He is a recipient of the IEEE Centennial Medal (1984), IEEE Canada's McNaughton Gold Medal (1995), the IEEE Haraden Pratt Award (1999), the IEEE Third Millennium Medal (2000), and the IEEE Graduate Teaching Award (2002). He is very active in the IEEE and was nominated by the IEEE Board of Director for the Office of IEEE President-Elect in the year 2002 election. Currently, he serves on the Board of the IEEE Information Theory and Communications societies. He is an Editor for the IEEE TRANSACTIONS ON COMMUNICATIONS and the IEEE TRANSACTIONS ON WIRELESS COMMUNICATIONS. He is a Past President of the IEEE Information Theory Society.